



# Multi-walled carbon nanotubes (MWCNTs)-bridged architecture of ternary $\text{Bi}_2\text{O}_3/\text{MWCNTs}/\text{Cu}$ microstructure composite with high catalytic performance via two-step self-assembly

Yafei Feng<sup>a,b</sup>, Heng Jiang<sup>b</sup>, Yuren Wang<sup>b,\*</sup>, Xiaoyan Jing<sup>a</sup>, Meng Chen<sup>b</sup>, Zheng Hu<sup>b</sup>, Tong Lu<sup>b</sup>

<sup>a</sup> Key Laboratory of Super-light Materials & Surface Technology, Ministry of Education, Harbin Engineering University, Harbin 150001, People's Republic of China

<sup>b</sup> Key Laboratory of Microgravity Science, Institute of Mechanics, Chinese Academy of Sciences, Beijing 100190, People's Republic of China

## ARTICLE INFO

### Article history:

Received 14 February 2012

Received in revised form

27 March 2012

Accepted 27 April 2012

Available online 23 May 2012

### Keywords:

Ternary microstructure composite

$\text{Bi}_2\text{O}_3/\text{MWCNTs}/\text{Cu}$

MWCNTs-bridged

Self-assembly

Ammonium perchlorate

## ABSTRACT

Binary and ternary microstructure composites based on CNTs have potential applications in many technological fields. In our works, we realized MWCNTs-bridged architecture of ternary  $\text{Bi}_2\text{O}_3/\text{MWCNTs}/\text{Cu}$  microstructure composite by two-step self-assembly. In order to verify its workability, we investigated catalytic performances of a series of additives for ammonium perchlorate (AP) thermal decomposition. The results showed that catalytic performance of  $\text{Bi}_2\text{O}_3/\text{MWCNTs}/\text{Cu}$  composite was better than those of the other additives, and the peak temperature for high-temperature AP decomposition reduced  $151.6^\circ\text{C}$ ; while no low-temperature AP decomposition was observed. MWCNTs have two crucial roles in catalytic enhancement on AP thermal decomposition: firstly, being to act as a supporter which can effectively disperse copper and  $\text{Bi}_2\text{O}_3$  particles; secondly, being to act as a bridge, excited electrons from semiconductor can conduct and store on the surfaces of MWCNTs, which is beneficial for AP thermal decomposition. Therefore, MWCNTs-bridged architecture can synergistically enhance catalytic effect of copper and  $\text{Bi}_2\text{O}_3$ .

© 2012 Elsevier Masson SAS. All rights reserved.

## 1. Introduction

Microstructure composites based on carbon nanotubes (CNTs) have potential applications in many fields, such as catalysis, hydrogen storage and sensors etc., because CNTs can improve performances of the composites [1–8]. In the studies of composite catalysts, CNTs can be used as dispersing-supporters, which can effectively disperse nanoparticles and enhance the catalytic activity, thus CNTs-based composite catalysts have attracted much research interest. But related researches have been usually focused on binary composite catalysts [9–13]. More recently, CNTs-based ternary composite catalysts have been initially investigated by some teams. Khanderi et al. [14] found that introducing ZnO into Au/MWCNT binary composite can increase the selectivity towards C=O group hydrogenation of Au/MWCNT catalysts. Chu and co-workers [15] reported that Pd– $\text{In}_2\text{O}_3/\text{CNTs}$  exhibited higher activity for ethanol oxidation than Pd/CNTs. Wang et al. [16] also demonstrated that the catalytic activity of Pt– $\text{CeO}_2/\text{CNTs}$  can be improved by adsorbing Pt nanoparticles on  $\text{CeO}_2/\text{CNTs}$ . These investigations demonstrated that the catalytic performances of CNTs-based binary composites

could be further improved by introducing a third phase. However, except for utilizing CNTs to serve as supporters, electrical properties of CNTs have been rarely employed to substantially enhance synergistical performances inside ternary composites and achieve excellent functional microstructure composites. When CNTs act as bridges to realize molecular scale connection with metal and semiconductor, the excellent electron-storage and -transport properties of CNTs can enhance integral performance of ternary microstructure composite.

Here, we reported a two-step self-assembly approach to synthesize ternary microstructure composite multi-walled carbon nanotubes (MWCNTs) supporting bismuth oxide ( $\text{Bi}_2\text{O}_3$ ) nanoparticles on copper particles, the new material reported here was called ternary  $\text{Bi}_2\text{O}_3/\text{MWCNTs}/\text{Cu}$  microstructure composite. The synthesis processes of ternary  $\text{Bi}_2\text{O}_3/\text{MWCNTs}/\text{Cu}$  microstructure composite were elaborately designed, aiming at utilizing carboxyl group on MWCNTs to realize MWCNTs-bridged architecture between Cu and  $\text{Bi}_2\text{O}_3$ . The first key problem was intentionally to choose greater scale copper particles in order to intuitively exhibit MWCNTs-bridged architecture in ternary  $\text{Bi}_2\text{O}_3/\text{MWCNTs}/\text{Cu}$  microstructure composite. The second was to modify copper and MWCNTs with amino and carboxyl, respectively. In this way, residual carboxyl group on MWCNTs provided growth site for  $\text{Bi}_2\text{O}_3$

\* Corresponding author. Tel.: +86 (0) 10 82544091; fax: +86 (0) 10 82544096.  
E-mail address: [yurenwang@imech.ac.cn](mailto:yurenwang@imech.ac.cn) (Y. Wang).

after copper assembled with MWCNTs. In order to verify availability of ternary  $\text{Bi}_2\text{O}_3/\text{MWCNTs}/\text{Cu}$  microstructure composite, we investigated its catalytic performance on ammonium perchlorate (AP). AP is an important oxidizer in solid propellants, which has been commonly used to investigate catalytic performances of materials. The catalytic results demonstrated that ternary  $\text{Bi}_2\text{O}_3/\text{MWCNTs}/\text{Cu}$  composite possessed excellent catalytic effect on AP thermal decomposition.

## 2. Experimental

### 2.1. Chemical reagents

Multi-walled carbon nanotubes (MWCNTs, >95%, diameter: from 50 nm to 100 nm) and copper particles (>99.7%, average diameter: 100 nm) were obtained from Nachen S&T Ltd. and Kunshan Miyou Nanotechnology Co., Ltd., respectively. 2-aminoethanethiol ( $\text{H}_2\text{N}(\text{CH}_2)_2\text{SH}$ , 95%) was purchased from J&K Scientific Ltd. The other chemicals are all reagent grade. All water used was purified with a Milli-Q plus system (Millipore Co.); the resistivity was over 18 M  $\Omega$  cm.

### 2.2. Synthesis of ternary $\text{Bi}_2\text{O}_3/\text{MWCNTs}/\text{Cu}$ microstructure composite

#### 2.2.1. Acid treatment of MWCNTs

0.2 g multi-walled carbon nanotubes (MWCNTs) were carboxyl-functionalized by acid treatment in 20 ml (1:3)  $\text{HNO}_3/\text{H}_2\text{SO}_4$  mixture, followed by ultrasonication for 4 h at 60 °C. The reaction mixture was diluted with ultrapure water until the suspension pH was nearly neutral. Then the suspension was centrifugated. The MWCNTs were collected and dried at 100 °C (Scheme 1(b)). (The details of functional groups on acid-treated MWCNTs were shown in Fig. S1 and Table S1.)

#### 2.2.2. Amino modification of copper particles

0.2 g copper particles were immersed in 5 mmol/L 2-aminoethanethiol ( $\text{H}_2\text{N}-(\text{CH}_2)_2-\text{SH}$ ) solution for 3 h at room temperature to form Cu–S bonds (Scheme 1(a)).

#### 2.2.3. Preparation of Cu/MWCNTs

A few drops of Tween 20 were spread in 0.3 mg/ml carboxyl-functionalized MWCNTs ethanol solution and sonicated for 30 min. Then copper particles with short chain ( $\text{H}_2\text{N}-\text{CH}_2-\text{CH}_2-\text{S}-$ ) and the carboxyl-functionalized MWCNTs

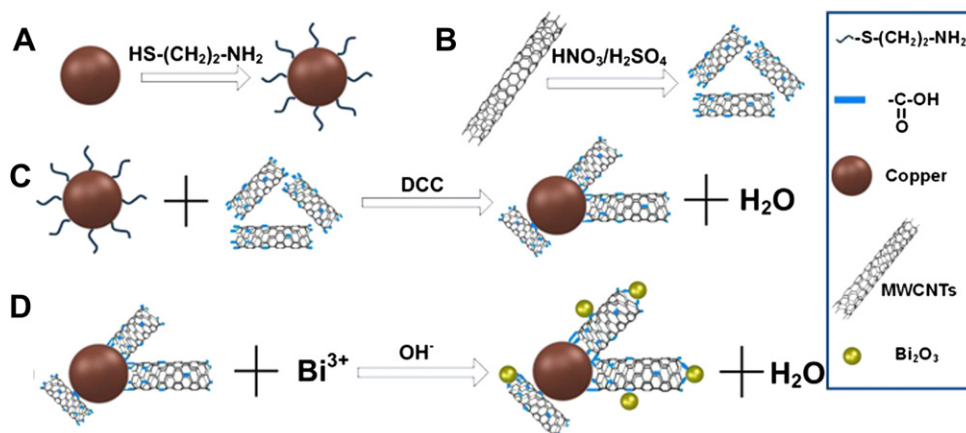
ethanol solution were mixed to assemble with the aid of 0.5 mg/ml dicyclohexylcarbodiimide (DCC) and stirred for 28 h at room temperature, after that MWCNTs were grown onto the surfaces of copper particles (Scheme 1(c)).

#### 2.2.4. Preparation of $\text{Bi}_2\text{O}_3/\text{MWCNTs}/\text{Cu}$

Firstly, 0.1 g  $\text{Bi}(\text{NO}_3)_3 \cdot 5\text{H}_2\text{O}$  was dissolved in 10% vol acetic acid solution by ultrasonication, the compound of Cu/MWCNTs was dispersed into the clear solution and stirred for 1 h at room temperature. Then, 30% wt sodium hydroxide solution was added dropwise into the above suspension solution to precipitate bismuth as bismuth oxide. Finally, bismuth oxide nanoparticles were grown onto MWCNTs which were based on copper particles. Then the products were diluted with ultrapure water and dried at 50 °C in vacuum (Scheme 1(d)).

### 2.3. Materials characterization and catalytic test

X-ray diffraction (XRD) patterns of ternary  $\text{Bi}_2\text{O}_3/\text{MWCNTs}/\text{Cu}$  microstructure composite were obtained on a Rigaku Ultima IV X-ray diffractometer with a Cu  $K\alpha_1$  radiation source ( $k = 1.54056 \text{ \AA}$ ) operated at 40 kV and 40 mA at a scanning step of  $0.01^\circ$  in the  $2\theta$  range  $10^\circ-80^\circ$ . The morphological and structural information of the studied  $\text{Bi}_2\text{O}_3/\text{MWCNTs}/\text{Cu}$  microstructure composite were obtained on a Philips CM-200 FEG transmission electron microscope (TEM) with an accelerating voltage of 200 kV and a JSM-6460 scanning electron microscope (SEM) with an energy dispersive spectrometer (EDS). To prepare six samples for the thermal decomposition experiments: (a) is pure AP; (b) is AP with  $\text{Bi}_2\text{O}_3/\text{MWCNTs}$  composite, the SEM image of  $\text{Bi}_2\text{O}_3/\text{MWCNTs}$  composite was shown in Fig. S3; (c) is AP with Cu/MWCNTs composite, the SEM image of Cu/MWCNTs composite was shown in Fig. S4; (d) is AP with  $\text{Bi}_2\text{O}_3/\text{MWCNTs}/\text{Cu}$  composite; (e) is mixture of AP and  $\text{Bi}_2\text{O}_3$ , the XRD pattern of  $\text{Bi}_2\text{O}_3$  powders was shown in Fig. S2; (f) is mixture of AP and Cu. The content of AP is about 98% by weight in each sample (from sample (b) to (f)). Thermal decomposition studies were performed with the Perkin–Elmer DSC-7 differential scanning calorimeter under an atmosphere of  $\text{N}_2$  (at a rate of 20 ml/min), from 20 °C to 500 °C and with a heating rate of 20  $\text{K min}^{-1}$ . In order to avoid nonuniform mix, the mixture of 14.7 mg AP and 0.3 mg catalyst was prepared at one time for DSC testing. The accuracy of the balance is 0.01 mg. And new ceramic crucible was essentially used every time. To ensure the reliability of catalytic performance, every kind of catalysts was carried out DSC test for three times.



**Scheme 1.** Preparation processes of ternary  $\text{Bi}_2\text{O}_3/\text{MWCNTs}/\text{Cu}$  microstructure composite: (a) surface modification of copper particles, (b) acid treatment of multi-walled carbon nanotubes, (c) self-assembly of copper particles and multi-walled carbon nanotubes, (d) preparation of  $\text{Bi}_2\text{O}_3$  nanoparticles on Cu/MWCNTs.

### 3. Results and discussion

Some typical microscopic images of ternary  $\text{Bi}_2\text{O}_3/\text{MWCNTs}/\text{Cu}$  microstructure composite and acid-treated MWCNTs are shown in Fig. 1. Fig. 1(a) shows acid-treated MWCNTs. Fig. 1(b) shows MWCNTs were nucleated and grown along the surfaces of copper particles so that most of the edges of these particles formed facets of uneven crystal growth (the details also can be seen in Fig. 1(c)). Only a few edges of copper particles were smooth due to the absence of MWCNTs, as indicated by a spotted curved line in Fig. 1(b). The covalent attachment of copper particles and MWCNTs strongly coupled together. Similar experiments had been done by other groups [17–19].  $\text{Bi}_2\text{O}_3$  nanoparticles were observed on MWCNTs, in comparison with the diameter of acid-treated MWCNTs (Fig. 1(a)). Fig. 1(b) demonstrated that designed self-assembly processes of ternary  $\text{Bi}_2\text{O}_3/\text{MWCNTs}/\text{Cu}$  microstructure composite were feasible and reasonable, MWCNTs-bridged architecture had been realized. It can be clearly seen that MWCNTs were effective in dispersing copper particles and  $\text{Bi}_2\text{O}_3$  nanoparticles, a uniform distribution of copper particles can be seen in Fig. 1(c).

XRD investigation for ternary  $\text{Bi}_2\text{O}_3/\text{MWCNTs}/\text{Cu}$  microstructure composite is reported in Fig. 2. All the primary diffraction peaks corresponded to Cu and monoclinic bismite  $\text{Bi}_2\text{O}_3$  (space group:  $P2_1/c$ ; lattice constant:  $a_0 = 5.84 \text{ \AA}$ ,  $b_0 = 8.16 \text{ \AA}$  and  $c_0 = 7.49 \text{ \AA}$ ; JCPDS file no. 65–2366), the average  $\text{Bi}_2\text{O}_3$  particle size was estimated to be 66 nm by the Sherrer formula. And impurity diffraction peaks from copper oxide were also detected owing to oxidation during the processes of storage and preparation. The diffraction peaks from the MWCNTs supporters cannot be

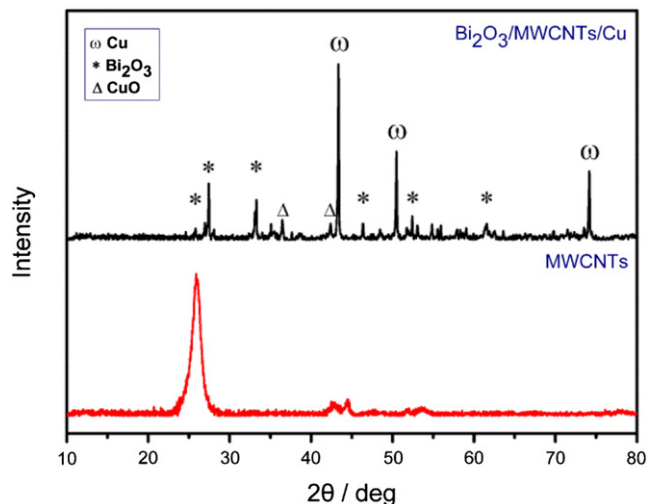


Fig. 2. XRD patterns of  $\text{Bi}_2\text{O}_3/\text{MWCNTs}/\text{Cu}$  microstructure composite and MWCNTs.

observed, because of the minute quantity of MWCNTs contained in the sample and an overwhelming diffraction signal from the  $\text{Bi}_2\text{O}_3$  phase [20].

Fig. 3 shows the processes of AP thermal decomposition and catalytic effects of different catalysts for AP thermal decomposition. The AP thermal decomposition process has three characteristic peaks (Fig. 3(a)). The endothermic DSC peak at  $249.8 \text{ }^\circ\text{C}$  represents a transition from orthorhombic to cubic. The AP thermal decomposition occurs in two steps: the first exothermic peak at  $342 \text{ }^\circ\text{C}$

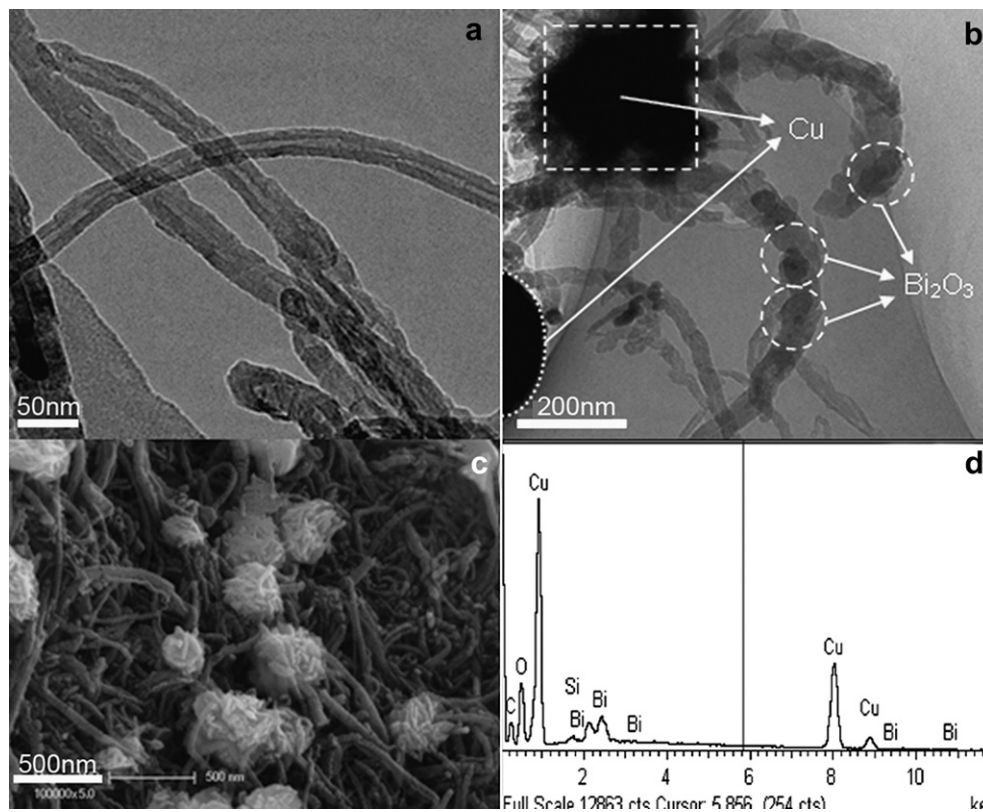
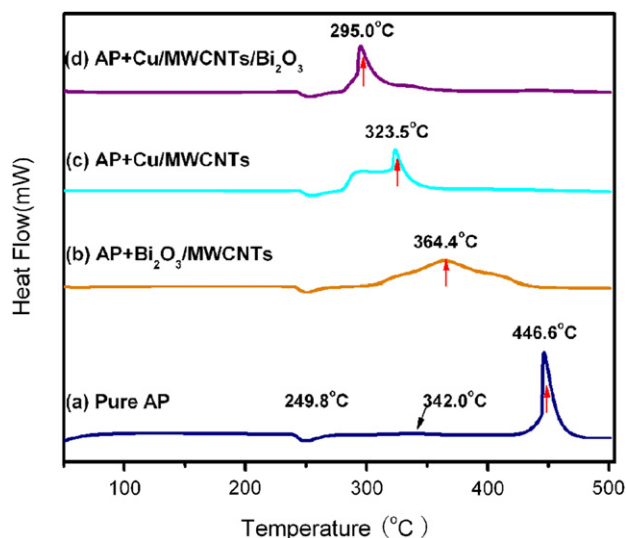


Fig. 1. Images of the samples, (a) TEM image of acid-treated MWCNTs, (b) TEM image of  $\text{Bi}_2\text{O}_3/\text{MWCNTs}/\text{Cu}$  microstructure composite: the uneven copper particle and  $\text{Bi}_2\text{O}_3$  particles are indicated by the dashed rectangle and dashed circle, respectively; the smooth copper particle is indicated by the spotted arc, (c) SEM image of  $\text{Bi}_2\text{O}_3/\text{MWCNTs}/\text{Cu}$  microstructure composite, (d) EDS of  $\text{Bi}_2\text{O}_3/\text{MWCNTs}/\text{Cu}$  microstructure composite. The elements on the sample surface are Cu, C, O and Bi. Si element comes from the silicon substrate which was used to disperse the sample.



**Fig. 3.** DSC patterns of different samples: (a) pure AP, (b) AP and  $\text{Bi}_2\text{O}_3/\text{MWCNTs}$  composite, (c) AP and Cu/MWCNTs composite, (d) AP and  $\text{Bi}_2\text{O}_3/\text{MWCNTs}/\text{Cu}$  microstructure composite.

represents low-temperature AP decomposition; the main exothermic peak at  $446.6^\circ\text{C}$  represents high-temperature AP decomposition. When catalyst particles were added, there was no variation in crystal form transformation temperature, but all peaks of low-temperature AP decomposition disappeared or decreased; the peaks for high-temperature AP decomposition decreased to different degree (Details can be seen in Fig. 3(b)–(d) and Fig. S5(b)–(c)). The lower the decomposition temperature decreases, the better the catalytic effect is [21]. Compared with a single constituent catalyst or binary composite catalysts, the catalytic effect of ternary  $\text{Bi}_2\text{O}_3/\text{MWCNTs}/\text{Cu}$  composite was the best with the high-temperature peak for AP decomposition decreasing by  $151.6^\circ\text{C}$  (Details can be seen in Fig. 3(b)–(d) and Fig. S5(b)–(c)). In addition, the Figs. S3 and S5 show that the catalytic effects of the composites were superior to those of single constituent catalyst. Furthermore, compared with the binary catalysts of  $\text{Bi}_2\text{O}_3/\text{MWCNTs}$  and  $\text{Cu}/\text{MWCNTs}$ , ternary  $\text{Bi}_2\text{O}_3/\text{MWCNTs}/\text{Cu}$  composite possessed better catalytic effect (details can be seen in Fig. 3(b)–(d)). All of above results strongly supported that  $\text{Bi}_2\text{O}_3/\text{MWCNTs}/\text{Cu}$  microstructure composite had synergistically catalytic effect due to realization of molecular scale connection among MWCNTs,  $\text{Bi}_2\text{O}_3$  and Cu. In the  $\text{Bi}_2\text{O}_3/\text{MWCNTs}/\text{Cu}$  microstructure composite, copper and  $\text{Bi}_2\text{O}_3$  are metal and semiconductor metal oxide catalysts, respectively; their catalytic mechanisms had been reported previously [22,23]. However, these mechanisms cannot sufficiently explain the excellent catalytic effect of ternary  $\text{Bi}_2\text{O}_3/\text{MWCNTs}/\text{Cu}$  microstructure composite.

When copper and  $\text{Bi}_2\text{O}_3$  grow on MWCNTs, they can be effectively dispersed on MWCNTs dispersing-supporters, which can prevent the agglomeration of copper particles and as-formed  $\text{Bi}_2\text{O}_3$  particles, thus downsizing  $\text{Bi}_2\text{O}_3$  particles to nanoscales (As shown in Fig. 1(b) and (c)). Because nanoparticles possess large specific surface area and high catalysis activity, AP decomposition products can directly make contact with the reaction centres of the catalyst. In addition, electron-storage and -transport properties of CNTs can further improve catalytic performance of the composite [24].  $\text{Bi}_2\text{O}_3$  semiconductor can produce excited carriers under heat [25]. During AP thermal decomposition, the excited carriers will be transported from semiconductor to CNTs due to the interfacial effect in semiconductor [26–28]. If excited electrons store in MWCNTs, according

to the literature [29], AP adsorbed on MWCNTs will release oxygen, that is, stored electrons in MWCNTs can accelerate AP thermal decomposition. On the other hand, the products of AP thermal decomposition are various gases, such as  $\text{O}_2$ ,  $\text{NO}$ ,  $\text{Cl}_2$  and so on [30]. Copper can react with most of these gases, and the products are copper oxide and chloride, which are catalysts for AP [31]. When copper gradually turn into copper semiconductor oxide, excited electrons can continually transport to MWCNTs, then AP thermal decomposition can continuously carry out. In this paper, MWCNTs are to act as bridges on which copper and  $\text{Bi}_2\text{O}_3$  particles grow and unite, MWCNTs-bridged architecture can sufficiently contact with AP, which is beneficial for AP thermal decomposition. Storage and transport of the excited carriers along MWCNTs can improve the synergistically catalytic effect of copper and  $\text{Bi}_2\text{O}_3$  during AP thermal decomposition. Thus, as supporters and bridges, MWCNTs enable  $\text{Bi}_2\text{O}_3/\text{MWCNTs}/\text{Cu}$  composite to possess excellent catalytic effect, which attributed to realize MWCNTs-bridged architecture and molecular scale connection among Cu, MWCNTs and  $\text{Bi}_2\text{O}_3$  by a two-step self-assembly techniques.

#### 4. Conclusions

In summary, by utilizing MWCNTs as supporters and bridges,  $\text{Bi}_2\text{O}_3/\text{MWCNTs}/\text{Cu}$  microstructure composite with excellent catalytic performance was developed by a two-step self-assembly approach which is simple for preparing complex composite with different species, sizes and functions. The  $\text{Bi}_2\text{O}_3/\text{MWCNTs}/\text{Cu}$  microstructure composite enable the peak temperature for high-temperature AP decomposition to reduce  $151.6^\circ\text{C}$ . The catalytic results of ternary  $\text{Bi}_2\text{O}_3/\text{MWCNTs}/\text{Cu}$  composite for AP thermal decomposition demonstrated that electron-storage and -transport properties of MWCNTs substantially enhanced catalytic performance of the composite, when MWCNTs acted as bridges to realize molecular scale connection with Cu and  $\text{Bi}_2\text{O}_3$ . Ternary  $\text{Bi}_2\text{O}_3/\text{MWCNTs}/\text{Cu}$  microstructure composite gave a clue to design new microstructures through utilizing properties of CNTs to combine with different functional materials. In addition to catalysis, this original design concept can also be extended to other application areas, such as energy, sensor and stealthy technique.

#### Acknowledgments

We acknowledge Project supported by the State Key Development Program for Basic Research of China (Grant No. 2011CB710901), China Postdoctoral Science Foundation (Grant No. 20100480484) and Chinese Academy of Sciences K. C. Wong Post-doctoral Fellowships.

#### Appendix A. Supplementary material

Supplementary material associated with this article can be found, in the online version, at doi:10.1016/j.solidstatesciences.2012.04.038.

#### References

- [1] J.E. Huang, D.J. Guo, Y.G. Yao, H.L. Li, J. Electroanal. Chem. 577 (2005) 93–97.
- [2] X. Chen, P. Lukaszczuk, C. Tripisciano, M.H. Rummeli, J. Srensek-Nazzal, I. Pelech, R.J. Kalenczuk, E. Borowiak-Palen, Phys. Status Solidi B 247 (2010) 2664–2668.
- [3] A. Star, V. Joshi, S. Skarupo, D. Thomas, J.C.P. Gabriel, J. Phys. Chem. B 110 (2006) 21014–21020.
- [4] X. Fu, H. Yu, F. Peng, H. Wang, Y. Qian, Appl. Catal. A 321 (2007) 190–197.
- [5] S.J. Yang, J.H. Cho, K.S. Nahm, C.R. Park, Int. J. Hydrogen Energy 35 (2010) 13062–13067.
- [6] K.H. An, S.Y. Jeong, H.R. Hwang, Y.H. Lee, Adv. Mater. 16 (2004) 1005–1009.
- [7] T.X. Liu, I.Y. Phang, L. Shen, S.Y. Chow, W.D. Zhang, Macromolecules 37 (2004) 7214–7222.

- [8] Y. Geng, M.Y. Liu, J. Li, X.M. Shi, J.K. Kim, *Compos. Part A: Appl. Sci. Manuf.* 39 (2008) 1876–1883.
- [9] S.F. Zheng, J.S. Hu, L.S. Zhong, L.J. Wan, W.G. Song, *J. Phys. Chem. C* 111 (2007) 11174–11179.
- [10] W. Wang, P. Serp, P. Kalck, J.L. Faria, *Appl. Catal. B* 56 (2005) 305–312.
- [11] G.W. Yang, G.Y. Gao, C. Wang, C.L. Xu, H.L. Li, *Carbon* 46 (2008) 747–752.
- [12] X.J. Zhang, W. Jiang, D. Song, J.X. Liu, F.S. Li, *Mater. Lett.* 62 (2008) 2343–2346.
- [13] C. Ping, F. Li, Z. Jian, J. Wei, *Propell. Explos. Pyrot.* 31 (2006) 452–455.
- [14] J. Khanderi, R.C. Hoffmann, J. Engstler, J.J. Schneider, J. Arras, P. Claus, G. Cherkashinin, *Chem. Eur. J.* 16 (2010) 2300–2308.
- [15] D. Chu, J. Wang, S. Wang, L. Zha, J. He, Y. Hou, Y. Yan, H. Lin, Z. Tian, *Catal. Commun.* 10 (2009) 955–958.
- [16] J.S. Wang, J.Y. Xi, Y.X. Bai, Y. Shen, J. Sun, L.Q. Chen, W.T. Zhu, X.P. Qiu, *J. Power Sources* 164 (2007) 555–560.
- [17] L. Minati, G. Speranza, S. Torrenco, L. Toniutti, C. Migliaresi, D. Maniglio, M. Ferrari, A. Chiasera, *Surf. Sci.* 604 (2010) 1414–1419.
- [18] Z. Liu, Z. Shen, T. Zhu, S. Hou, L. Ying, *Langmuir* 16 (2000) 3569–3573.
- [19] E. Unger, G.S. Duesberg, M. Liebau, A.P. Graham, R. Seidel, F. Kreupl, W. Hoenlein, *Appl. Phys. A: Mater. Sci. Process* 77 (2003) 735–738.
- [20] J. Li, S. Tang, L. Lu, H. Zeng, *J. Am. Chem. Soc.* 129 (2007) 9401–9409.
- [21] L. Zhao, Z. Wang, D. Han, D. Tao, G. Guo, *Mater. Res. Bull.* 44 (2009) 984–988.
- [22] L. Liu, F. Li, L. Tan, L. Ming, Y. Yi, *Propellants, Explos., Pyrotech.* 29 (2004) 34–38.
- [23] G. Singh, I.P.S. Kapoor, S. Dubey, P.F. Siril, *J. Sci. Conf. Proc.* 1 (2009) 11–17.
- [24] Y.J. Xu, Y. Zhuang, X. Fu, *J. Phys. Chem. C* 114 (2010) 2669–2676.
- [25] D.A. Neamen, *Semiconductor Physics and Devices: Basic Principles*, third ed., McGraw-Hill Higher Education, New York, 2003, Chapter 6.
- [26] M. Long, W. Cai, H. Kisch, *J. Phys. Chem. C* 112 (2008) 548–554.
- [27] X. Zhao, H. Liu, J. Qu, *Appl. Surf. Sci.* 257 (2011) 4621–4624.
- [28] L. Fu, Z. Liu, Y. Liu, B. Han, P. Hu, L. Cao, D. Zhu, *Adv. Mater.* 17 (2005) 217–221.
- [29] L. Li, X. Sun, X. Qiu, J. Xu, G. Li, *Inorg. Chem.* 47 (2008) 8839–8846.
- [30] V.V. Boldyrev, *Thermochim. Acta* 443 (2006) 1–36.
- [31] J. Wang, S. He, Z. Li, X. Jing, M. Zhang, Z. Jiang, *Colloid Polym. Sci.* 287 (2009) 853–858.